OAK RIDGE NATIONAL LABORATORY
OPERATED BY
UNION CARBIDE CORPORATION
NUCLEAR DIVISION
POST OFFICE BOX X
OAK RIDGE, TENNESSEE 37830

ORNL/MIT-253

DATE: April 25, 1977 COPY NO.

SUBJECT: Flooding and Mass Transfer in Goodloe-Packed Columns, Part 2

Authors: J.S. Ayala, B.W. Brian, and A.C. Sharon

Consultants: A.D. Ryon, J.M. Begovich, and G.L. Haag

ABSTRACT

Flooding points and an overall mass transfer coefficient for Goodloe-packed columns were determined with a carbon dioxide-air-water system for 6.4 and 15.2-cm-ID columns. Flood points were obtained for liquid-to-gas mass velocity ratios of 20 to 800. A mixing model, assuming plug flow for the gas and dispersed flow for the liquid, was used to calculate an overall mass transfer coefficient, K_La. K_La, based on mass concentrations, ranged from 0.01 to 0.08 sec^{-1} and was found to increase with increasing liquid flow rate.

Oak Ridge Station
School of Chemical Engineering Practice
Massachusetts Institute of Technology
W.M. Ayers, Director

Contents

1. SUMMARY

Flooding points were determined in 6.4 and 15.2-cm-ID Goodloe-packed columns for liquid-to-gas mass velocity ratios of 20 to 800. The water flow rate was insufficient to flood a 27.9-cm-ID column. Tracer experiments performed in the 15.2-cm-ID column yielded Peclet numbers for the liquid of 11 to 25. Mass Transfer experiments, performed in each column, utilized a countercurrent flow of 4 to 5% carbon dioxide in air and water. However, data for the 27.9-cm-ID column was inconsistent with a mass balance and was therefore discarded. The inlet and outlet gas concentrations were measured with a gas chromatograph and the water-carbon dioxide concentration was measured by a titration. A model assuming plug flow for the gas and dispersed flow for the liquid was used to calculate the overall mass transfer coefficient, K_La. K_La was found to increase with increased liquid flow. There was little dependence of K_La on column diameter.

2. INTRODUCTION

Krypton gas is recovered from HTGR off-gas streams by countercurrent absorption in liquid carbon dioxide. Goodloe stainless steel wire mesh packing (10) was chosen for the absorption columns since the process operates at -20°C and about 20 atm pressure. To facilitate future column design, the hydrodynamics and mass transfer within Goodloe-packed columns are required. Choi *et al.* (4) investigated flooding in Goodloe-packed columns for air-water countercurrent flow and Chao *et al.* (3) investigated both flooding and mass transfer of carbon dioxide in air to water with the packing for liquid-to-gas mass velocity ratios of 1 to 23 in a 6.35-cm-ID column and 2 to 10 in a 15.2-cm-ID column. The present study determined the flooding points in two columns of the same diameter for liquid-to-gas mass velocity ratios of 20 to 800 which approximate the ratios in the krypton/liquid carbon dioxide system. In addition, a mass transfer coefficient for the absorption of carbon dioxide in water was investigated as a function of liquid and gas flow rates. Although, as with past investigations, the gas phase was assumed to be in plug flow, dispersion in the liquid phase, and hence the Peclet number, was experimentally determined prior to calculation of the mass transfer coefficient.

2.1 Objectives

The objectives were:

1. To experimentally determine the flooding points for the 6.4- and 15.2-cm-ID columns at liquid-to-gas superficial mass velocity ratios of 20 to 800.

2. To experimentally determine the liquid phase Peclet number.

3. To calculate mass transfer coefficient and investigate its dependence on gas and liquid flow rate.

2.2 Method of Attack

The flooding points were determined for liquid-to-gas superficial mass velocity ratios of 20, 50, 100, 200, 400, and 800 to simulate the liquid-to-gas flow rates used in the low temperature KALC process. The flooding curve was generalized for any fluid system and column diameter with a generalized correlation similar to the Eckert Correlation (6). Pressure drops through the two columns and pressure profiles along the length of the columns were also determined.

The Peclet number for the liquid phase was determined through tracer studies in the 15.2-cm-ID column with the analysis of moments method (7). Mass transfer coefficients were then calculated with the assumption of no dispersion (plug flow) in the gas phase and dispersion proportional to the experimentally determined Peclet number in the liquid phase. These calculations were performed for L/G mass ratios of 20, 50, 100, 200. 400, and 800 at 80% of the gas flow rate necessary for flooding.

3. DETERMINATION OF MASS TRANSFER COEFFICIENTS

To calculate the mass transfer from the gas to the liquid and to evaluate the overall mass transfer coefficients, it was necessary to relate the gas and liquid concentrations within the column to the inlet and outlet concentrations, flow rates, and dispersion within the column. Miyauchi has developed a model for countercurrent mass transfer that provides relations between these parameters (9). This model assumes a constant axial dispersion coefficient for each phase, E_G and E_L, and constant superficial velocities, U_G and U_L. Measuring the distance along the column, z, from the gas phase inlet, a steady state mass balance for the two phases yields:

$$E_G \frac{d^2C_G}{dz^2} - U_G \frac{dC_G}{dz} - K_G a(C_G - mC_L) = 0 \qquad (1)$$

$$E_L \frac{d^2C_L}{dz^2} + U_L \frac{dC_L}{dz} + K_L a(C_G - mC_L) = 0 \qquad (2)$$

Following Miyauchi's development, Eqs. (1) and (2) can be written in dimensionless form,

$$\frac{1}{Pe_G}\frac{d^2C_G}{dz_*^2} - \frac{dC_G}{dz_*} - \frac{K_G aH}{U_G}(C_G - mC_L) = 0 \qquad (3)$$

$$\frac{1}{Pe_L}\frac{d^2C_L}{dz_*^2} + \frac{dC_L}{dz_*} + \frac{K_L aH}{U_L}(C_G - mC_L) = 0 \qquad (4)$$

As the Peclet numbers approach infinity, the effect of convection becomes much greater than that of dispersion and the column approaches a plug flow condition. At the other extreme, when the Peclet number approaches zero, the column approaches the behavior of a perfectly mixed vessel or CSTR. At intermediate Peclet numbers both convection and dispersion are important. This condition is termed dispersed flow.

Determination of the Peclet number requires experimental information. Concentration profiles would indicate the Peclet number range in the column but would not give an accurate numerical value. A better approach is to perform tracer experiments such as those described by Levenspiel (7). The Peclet number can be related to the variance in tracer concentration response curves. The variance, σ^2 is given by

$$\sigma^2 = \frac{\int_0^\infty t^2 c_i \, dt}{\int_0^\infty c_i \, dt} - \bar{t}^2 \qquad (5)$$

where the mean residence time, $\bar{t}$, is given by

$$\bar{t} = \frac{\int_0^\infty t \, c_i \, dt}{\int_0^\infty c_i \, dt} \qquad (6)$$

Converting to the dimensionless variance,

$$\sigma_\theta^2 = \frac{\sigma^2}{\bar{t}^2} \qquad (7)$$

Levenspiel states for a closed system,

$$\sigma_\theta^2 = \frac{2}{Pe_i} - \frac{2}{Pe_i^2}(1 - e^{-Pe_i}) \tag{8}$$

Having obtained σ_θ^2 and therefore the Peclet number, Eqs. (3) and (4) can be solved with appropriate boundary conditions. Because it was not possible to measure gas phase dispersion, plug flow was assumed. An experiment to estimate the gas phase Peclet number with no water in the column is discussed in Appendix 10.4. This assumption eliminates the first term in Eq. (3). The three required boundary conditions are:

$$\text{at } z_* = 0\text{:}\quad C_G = 1$$

$$\therefore \frac{dC_L}{dz_*} = 0 \tag{9}$$

and

$$\text{at } z_* = 1\text{:}$$

$$\frac{dC_L}{dz_*} = Pe_L(C_L' - C_{L_1}) \tag{10}$$

where:

$$C_L' = C_L \text{ at } z_* = 1 + \delta z_*$$

$$C_{L_1} = C_L \text{ at } z_* = 1 - \delta z_*$$

i.e., the liquid concentration just above and below the top of the bed to account for the concentration discontinuity introduced from assuming the liquid is in dispersed flow. The calculation procedure for K_La is discussed in Appendix 10.1.

4. APPARATUS AND PROCEDURE

4.1 Apparatus

The apparatus consists of three plexiglas columns (6.4, 15.2, and 27.9-cm-ID) packed with #316 stainless steel Goodloe wire mesh packing. Each column has 24 ports to which eight manometers can be connected. The gas flow is measured with one of three rotameters and is introduced at the bottom of the two smaller columns via a capped pipe containing four holes,

and at the bottom of the largest column via a sparging ring. Carbon dioxide gas, the flow rate of which is measured with a separate rotameter, is mixed with the air in a mixing tank to provide a uniform feed prior to introduction to the column. A schematic of the apparatus is presented in Fig. 1.

Water flow to the smallest column is measured with one of two rotameters and is delivered to the top of the column through a simple distributor. Pall rings are located above the packing to distribute the water feed evenly. Up to 56 liters/min of water can be fed to the top of either of the larger columns. A plexiglas disc distributor is mounted at the top of each of these columns, and water flows down through holes in the disc, while gas escapes through tubes which extend through the disc above the water level. Water exits the columns through a drain or a pump. The water flow rates through the smallest column are low enough so that only the gravity drain is necessary. However, to maintain a stable liquid level in the bottom of the column, a variable-height weir pot is included in the gravity drain. A pump removes the water from the larger columns. The water level at the bottom of the larger columns is maintained by adjusting a throttling valve in the line to the pump as well as adjusting the height of the weir pot. A Radiometer Copenhagen Automatic Titrator and a Traycor Model 550 Gas Chromatograph were available for determination of aqueous and vapor phase carbon dioxide concentrations.

4.2 Experimental Procedure

4.2.1 Flooding Point Determinations

The experimental procedure for determining the flooding points of the two smaller columns for liquid-to-gas mass flow rate ratios of 20 to 800 was similar to that of Chao *et al.* (3). The column was first completely filled with water and then drained. In most experiments the water flow rate was set and the gas flow rate was increased until flooding was observed. In the smallest column, however, several flooding points were determined by setting the gas flow rate and increasing the liquid flow rate until flooding was observed. Six manometers were connected to sampling ports of different heights along the column. The pressure at each port was recorded at each gas and liquid flow rate. Readings were taken after the pressures had stabilized for each change in liquid or gas flow rate. The time for stabilization was between 1 and 5 min. Water and air flows were stopped after each flooding point had been determined, and the column was allowed to drain for 5 to 10 min. A number of experiments were repeated to determine reproducibility of the results.

4.2.2 Mass Transfer Experiments

Mass transfer parameters were determined at eleven operating conditions on the two columns. A 4 to 5% carbon dioxide/air mixture was fed into the bottom of the column and water into the top at the desired flow rates. Samples were taken from the gas and liquid inlet streams at the start

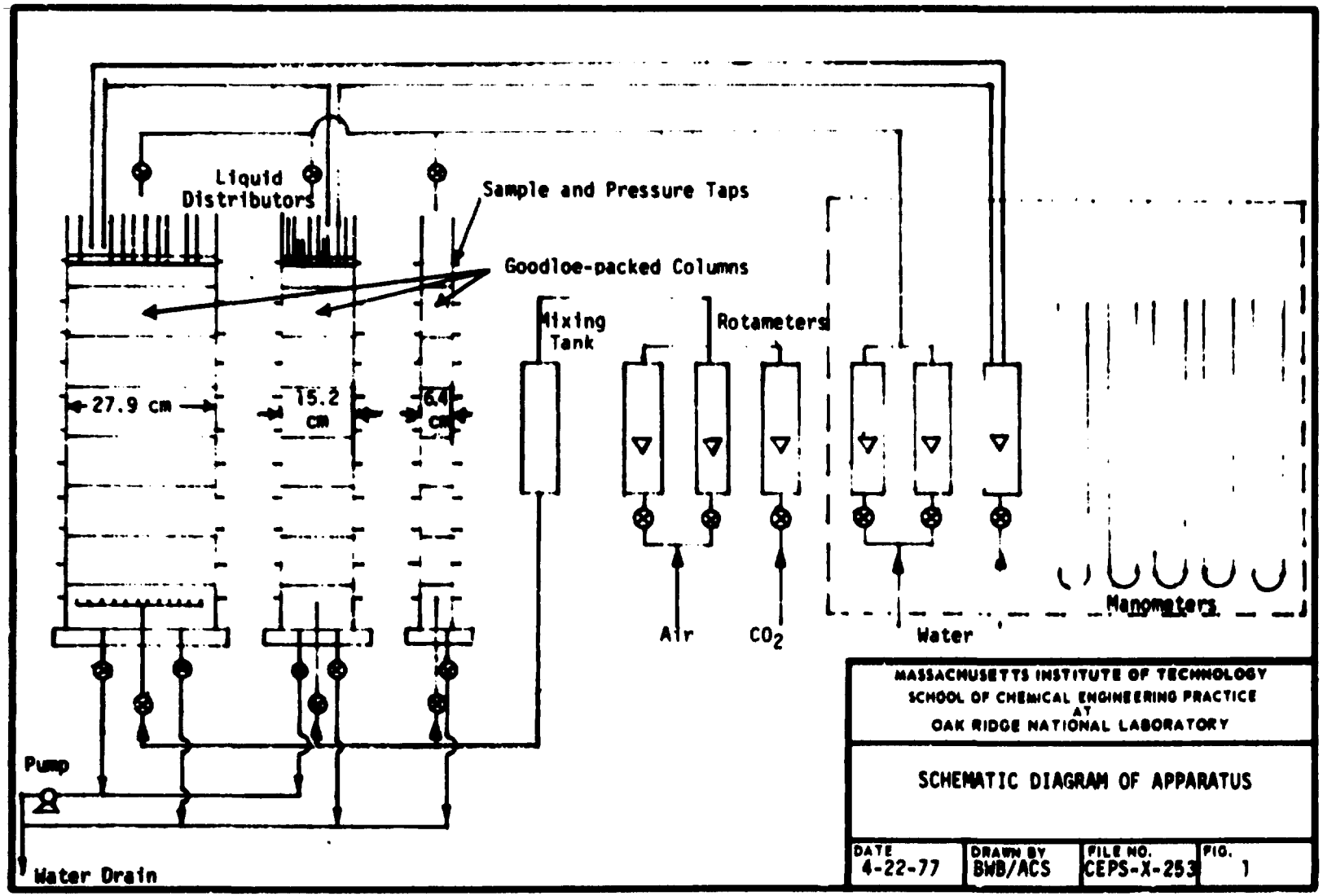
Liquid Distributors
Sample and Pressure Taps
Goodloe-packed Columns
Mixing Tank
Rotameters
27.9 cm
15.2 cm
6.4 cm
Air
CO_2
Water
Manometers
Pump
Water Drain
MASSACHUSETTS INSTITUTE OF TECHNOLOGY
SCHOOL OF CHEMICAL ENGINEERING PRACTICE
AT
OAK RIDGE NATIONAL LABORATORY
SCHEMATIC DIAGRAM OF APPARATUS
DATE 4-22-77
DRAWN BY BWB/ACS
FILE NO. CEPS-X-253
FIG. 1

and finish of each run and at 10-min intervals from both outlet streams until two consecutive samples yielded the same concentration. The column was considered at steady state at that time.

The gas phase concentration profile along the length of the column was determined for the largest and smallest columns with the method of Chao *et al.* (3). Samples were taken at twelve points in each column. The samples were then injected into the gas chromatograph to determine the carbon dioxide concentration.

Dispersion in the liquid phase was determined by quickly pouring fifty milliliters of a saturated potassium chloride solution into the liquid inlet of the column during a mass transfer run and recording the change in electrical conductivity of the outlet liquid with time. Since the concentration is proportional to the conductivity, the resulting data were analyzed to determine the Peclet number.

5. RESULTS AND DISCUSSION OF RESULTS

5.1 Flooding Experiments

The pressure profile in the 6.35-cm-ID column is nearly linear for all gas flow rates except near the bottom of the column at the highest gas rate prior to flooding (Fig. 2). This implies that the resistance to gas flow at constant liquid flow rates is uniform throughout the length of the column. As the gas flow rate is increased to nearly the rate necessary for flooding, the pressure drop across the bottom section of packing increases faster than that across the remainder of the column. This is due to loading, a phenomena which is similar to localized flooding, but which is visually observed as a stable liquid holdup in a section of the packing. Loading at the bottom of this column is due in part to the air distributor. Water passing through the column tended to drain from the bottom of the packing in sheets rather than in streams. Air introduced through four holes in the pipe distributor was blown radially outward from the center of the column. This air, especially at flow rates above 80% of those necessary for flooding, tended to blow sheets of water back into the packing, most markedly at the interface between the packing and the column wall.

The behavior displayed by the 15.2-cm-ID column is somewhat different from that of the smaller column (Fig. 3). The greatest pressure variation within the column is seen to take place across the bottom section of packing. This pressure variation results from the bottom segment of packing being loaded. The method of air feed to this column is similar to that of the smaller column, and the same water sheeting effect was noted under the bottom section of packing. As the gas flow rate increased, the pressure drop through the bottom section of packing and the height of the loaded section increased. Because of increased loading, hence increased resistance to gas flow, the pressure necessary for the gas to overcome the resistance is correspondingly greater. The column pressure profile

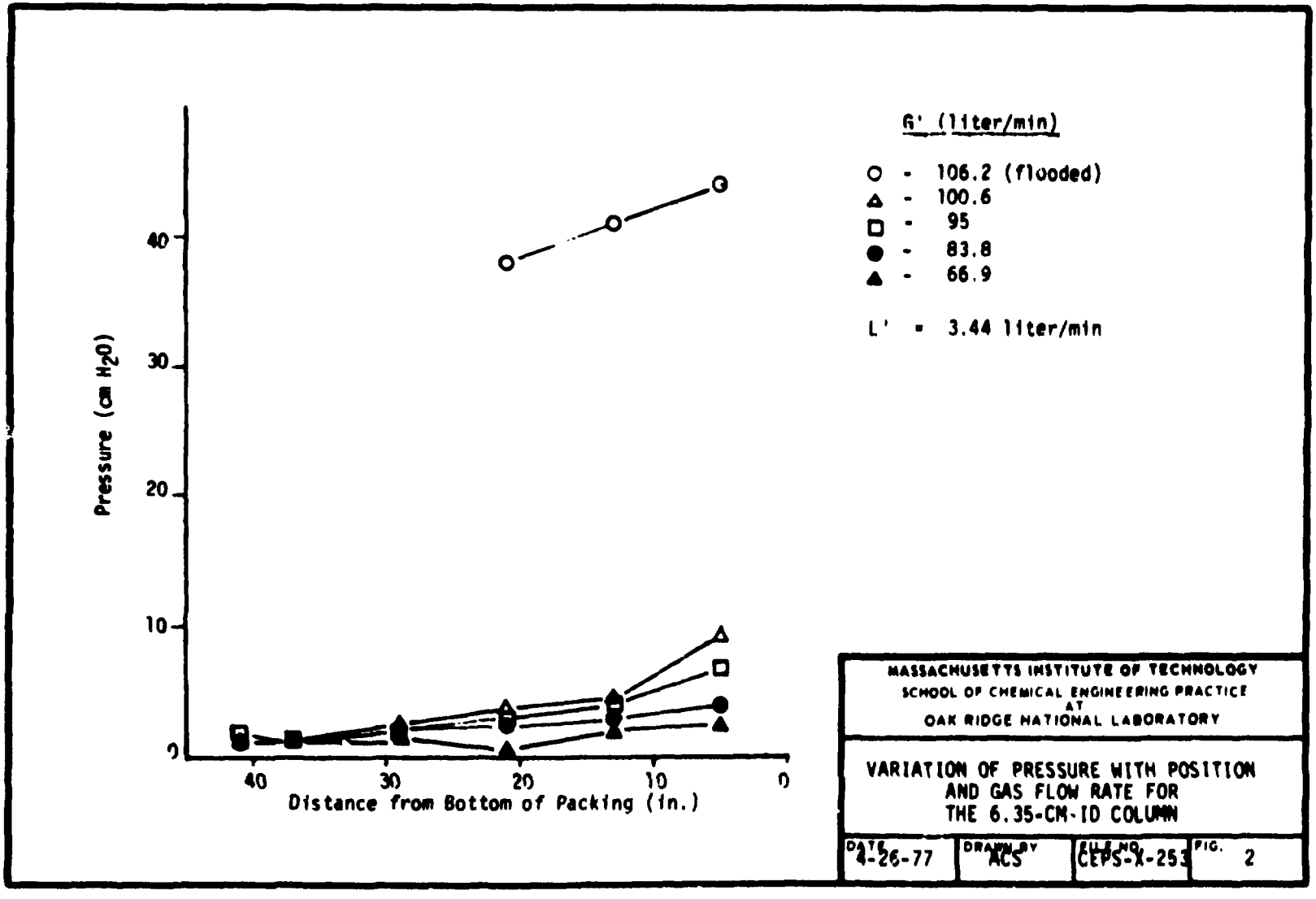
G' (liter/min)
○ - 106.2 (flooded)
△ - 100.6
□ - 95
● - 83.8
▲ - 66.9
L' = 3.44 liter/min
Pressure (cm H2O)
40
30
20
10
0
40
30
20
10
0
Distance from Bottom of Packing (in.)
MASSACHUSETTS INSTITUTE OF TECHNOLOGY
SCHOOL OF CHEMICAL ENGINEERING PRACTICE
AT
OAK RIDGE NATIONAL LABORATORY
VARIATION OF PRESSURE WITH POSITION
AND GAS FLOW RATE FOR
THE 6.35-CM-ID COLUMN
DATE 4-26-77
DRAWN BY ACS
FILE NO. CEPS-X-253
FIG. 2

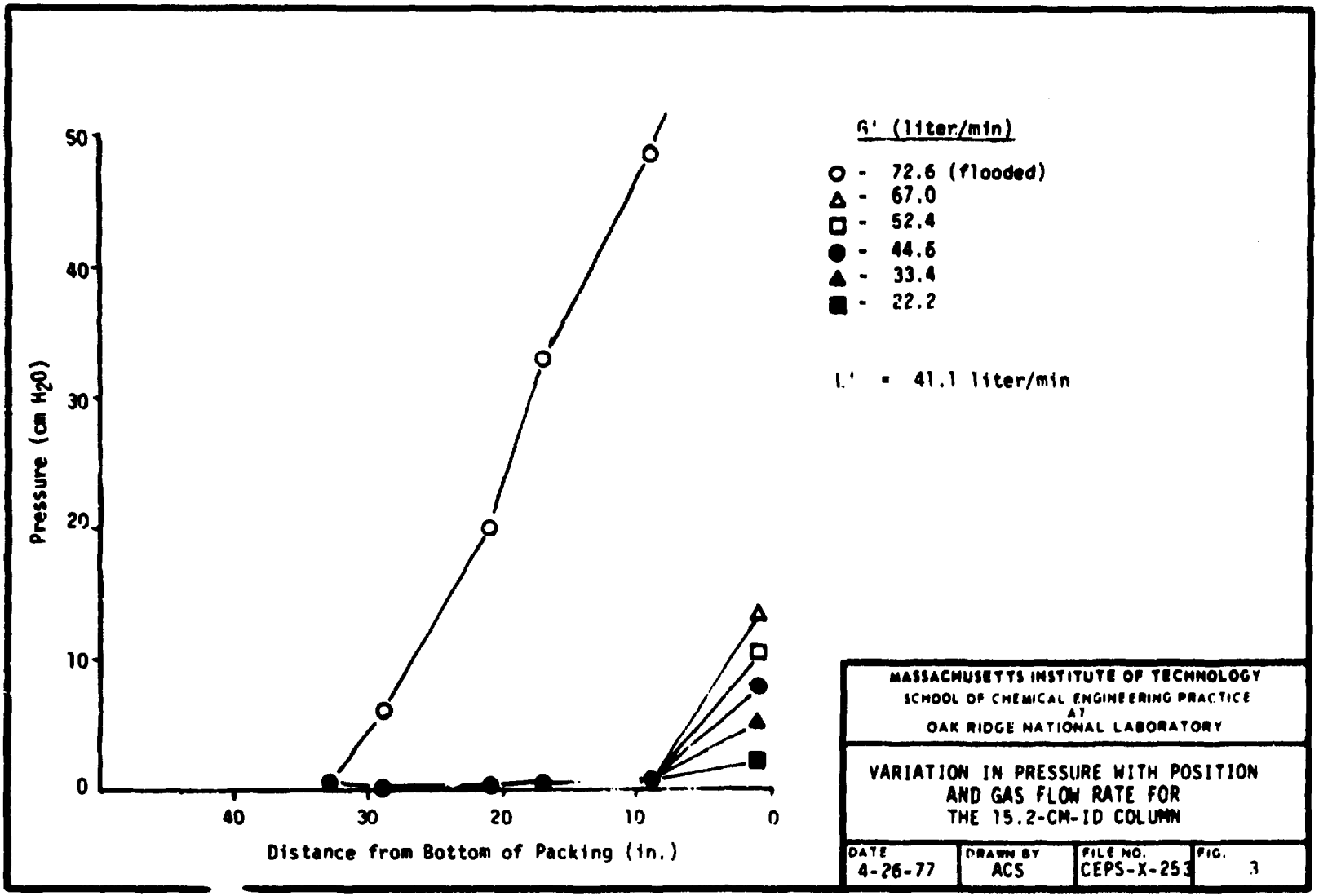
G' (liter/min)
○ - 72.6 (flooded)
△ - 67.0
□ - 52.4
● - 44.6
▲ - 33.4
■ - 22.2
L' = 41.1 liter/min
Pressure (cm H2O)
50
40
30
20
10
0
40
30
20
10
0
Distance from Bottom of Packing (in.)
MASSACHUSETTS INSTITUTE OF TECHNOLOGY
SCHOOL OF CHEMICAL ENGINEERING PRACTICE
AT
OAK RIDGE NATIONAL LABORATORY
VARIATION IN PRESSURE WITH POSITION
AND GAS FLOW RATE FOR
THE 15.2-CM-ID COLUMN
DATE 4-26-77
DRAWN BY ACS
FILE NO. CEPS-X-253
FIG. 3

at a lower liquid and greater gas flow rates is presented in Fig. 4. At low gas flow rates, a nearly linear pressure profile is observed, similar to the profile of the smaller column. As the gas flow rate is increased, large increases in the pressure drop through the column are observed. At a gas flow rate of 424 liter/min, a large linear pressure drop across the lower half of the column is observed. At a gas flow rate of 437 liter/min, a larger, uneven pressure drop is observed throughout the column, and at a gas flow rate of 445 liter/min, flooding occurs.

Corresponding to the large pressure drops across sections of the column were visual observations of loading in the sections. At a gas flow rate of 424 liter/min, the entire bottom section of packing and the lowest three quarters of the second section were loaded. At a gas flow rate of 437 liter/min, loading was observed in parts of the two top sections of packing as well as the bottom two sections.

The pressure drop through the 6.35-cm-ID column as a function of gas flow rate for several liquid flow rates is presented in Fig. 5. The highest point on a constant liquid flow rate curve corresponds to the looding point.

The pressure drop through the 15.2-cm-ID column as a function of gas flow rate for several liquid flow rates is presented in Fig. 6. The highest point on the constant liquid flow rate curves again corresponds to the flooding point. These curves are not uniform. The pressure drop through the column at gas flow rates less than those necessary for flooding is much greater than that for the 6.35-cm-ID column due to greater loading. At 20.4 and 12.2 liter/min, flooding was determined by visually observing liquid surging up through the packing rather than by monitoring the pressure drop.

The flooding points for both columns are reported in Fig. 7 in terms of the gas and liquid mass flux through the columns. Expressed in this manner, the same mass flux through a column was expected to yield the same flooding points if the packing in both columns exhibited the same resistance to liquid and gas flow. However, the 15.2-cm-ID column, except at the lowest gas flow rates, flooded at lower gas flow rates than the 6.4-cm-ID column. It has been suggested that the flooding characteristics of a column are very dependent on the condition of its packing (1). The greater resistance to gas and liquid flow in the larger column, especially at lower liquid flow rates, and the presence of loading at several positions in the column indicate a greater resistance to flow and possibly damage to the packing interface. Damaged packing might explain the observation of loading and flooding at lower than expected fluxes for the 15.2-cm-ID column. Examination of Fig. 7 indicates a nearly linear relation between the liquid and gas flux at which flooding occurs for L/G ratios greater than 20 and less than 400 for both columns. Once the 15.2-cm-ID column is repacked and the flooding points verified, such a correlation should be developed for each column.

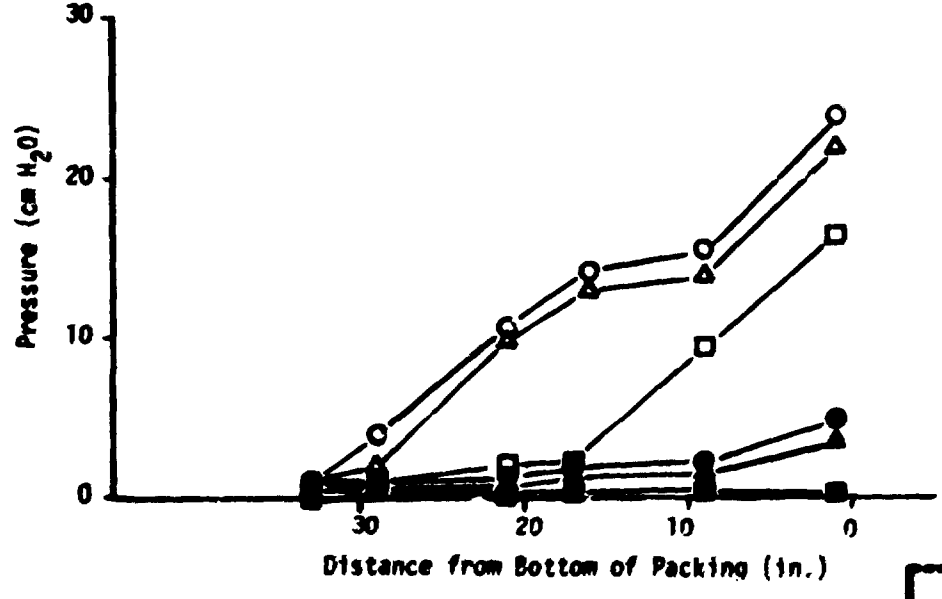

G' (liter/min)

- ○ - 445
- △ - 437
- □ - 424
- ● - 381
- ▲ - 317
- ■ - 78.2

L' = 12.2 liter/min

MASSACHUSETTS INSTITUTE OF TECHNOLOGY
SCHOOL OF CHEMICAL ENGINEERING PRACTICE
AT
OAK RIDGE NATIONAL LABORATORY

VARIATION OF PRESSURE WITH POSITION AND GAS FLOW RATE FOR 15.2-CM-ID COLUMN

DATE	DRAWN BY	FILE NO.	FIG.
4-26-77	ACS	CEPS-X-253	4

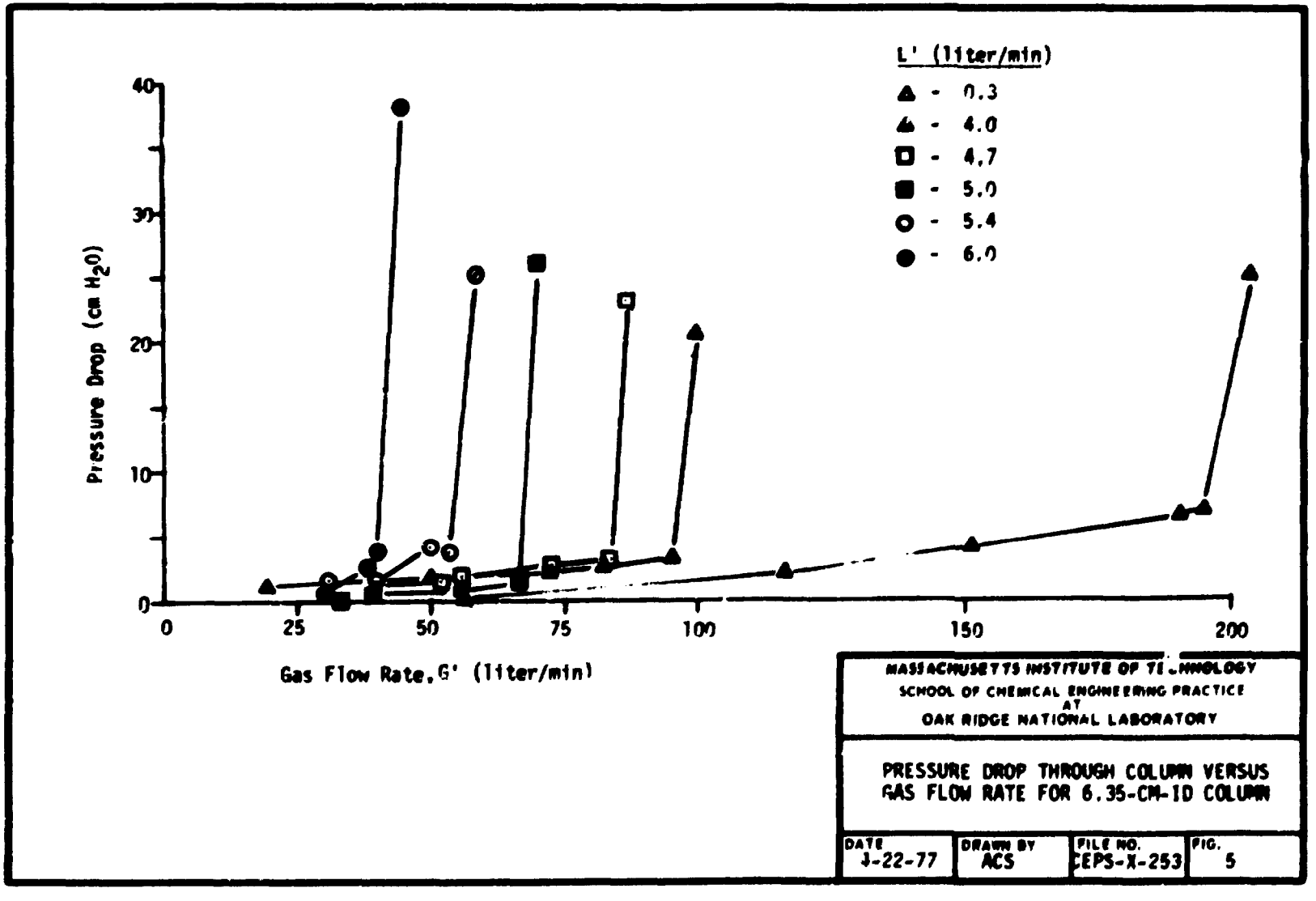
L' (liter/min)
▲ - 0.3
▲ - 4.0
□ - 4.7
■ - 5.0
○ - 5.4
● - 6.0
Pressure Drop (cm H_2O)
40
30
20
10
0
0
25
50
75
100
150
200
Gas Flow Rate, G' (liter/min)
MASSACHUSETTS INSTITUTE OF TECHNOLOGY
SCHOOL OF CHEMICAL ENGINEERING PRACTICE
AT
OAK RIDGE NATIONAL LABORATORY
PRESSURE DROP THROUGH COLUMN VERSUS GAS FLOW RATE FOR 6.35-CM-ID COLUMN
DATE J-22-77
DRAWN BY ACS
FILE NO. CEPS-X-253
FIG. 5

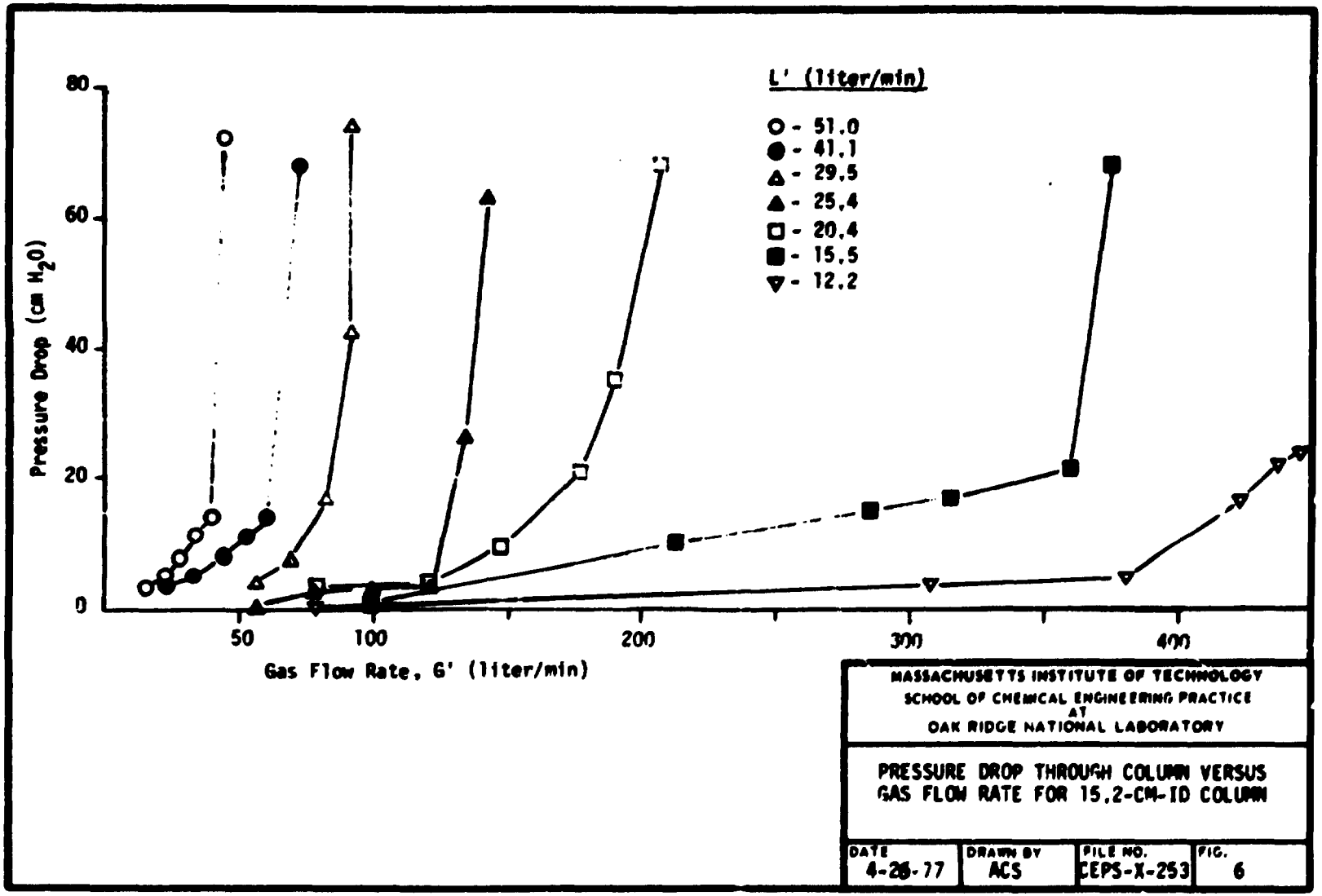
L' (liter/min)
○ - 51.0
● - 41.1
△ - 29.5
▲ - 25.4
□ - 20.4
■ - 15.5
▽ - 12.2
Pressure Drop (cm H_2O)
0
20
40
60
80
50
100
200
300
400
Gas Flow Rate, G' (liter/min)
MASSACHUSETTS INSTITUTE OF TECHNOLOGY
SCHOOL OF CHEMICAL ENGINEERING PRACTICE
AT
OAK RIDGE NATIONAL LABORATORY
PRESSURE DROP THROUGH COLUMN VERSUS GAS FLOW RATE FOR 15.2-CM-ID COLUMN
DATE 4-26-77
DRAWN BY ACS
FILE NO. CEPS-X-253
FIG. 6

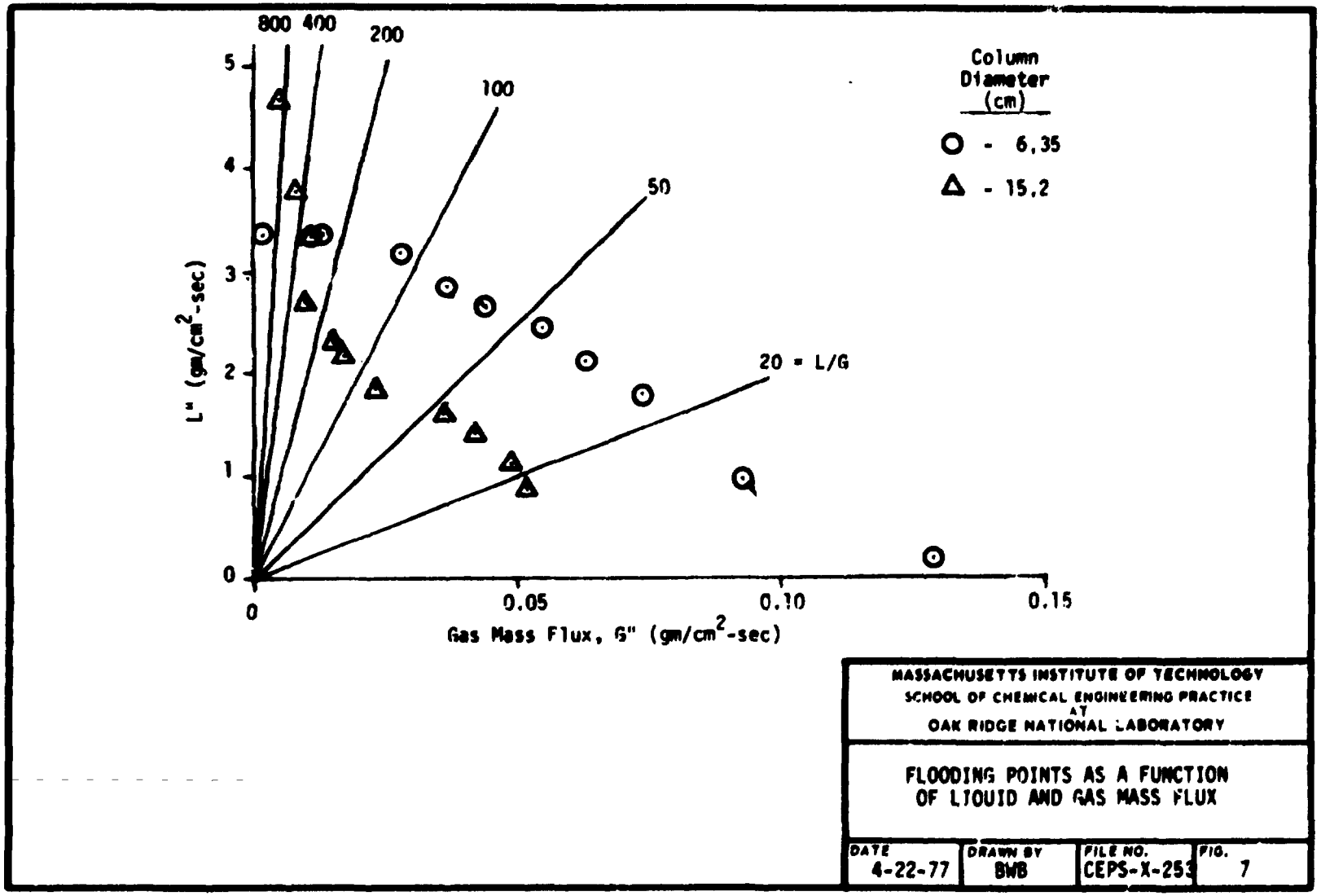
800
400
200
100
50
20 = L/G
Column Diameter (cm)
O - 6.35
Δ - 15.2
L" (gm/cm²-sec)
Gas Mass Flux, G" (gm/cm²-sec)
0
1
2
3
4
5
0.05
0.10
0.15
MASSACHUSETTS INSTITUTE OF TECHNOLOGY
SCHOOL OF CHEMICAL ENGINEERING PRACTICE
AT
OAK RIDGE NATIONAL LABORATORY
FLOODING POINTS AS A FUNCTION OF LIQUID AND GAS MASS FLUX
DATE 4-22-77
DRAWN BY BWB
FILE NO. CEPS-X-253
FIG. 7

A generalized flooding point correlation is presented in Fig. 8. It contains flooding points for Goodloe-packed columns reported by several previous investigators (1, 3, 4), as well as the current data and the manufacturer's correlation (10). The present work considerably extends the range of liquid and gas flow rates at which flooding has been reported. The results obtained from this work seem to indicate that flooding occurs at somewhat higher flow rates for the 6.4-cm-ID column than reported by others. For the 15.2-cm-ID column, the results very nearly correspond to those in previous work. The parameters in Fig. 8 are explained in Appendix 10.2.1.

5.2 Dispersion and Mass Transfer Coefficients

Peclet numbers for the liquid phase were obtained at eleven liquid/gas flow rates for the 15.2-cm-ID column (Fig. 9). Two residence time distribution curves were obtained for each condition, with the smoother of the two curves used to calculate the Peclet number. The liquid Peclet numbers ranged from 11.1 to 25.8, indicative of intermediate dispersion. Therefore, the plug flow assumption for the liquid phase made in previous studies is not justified. From Fig. 9, no clear relation can be obtained between the liquid Peclet number and either the gas or liquid flow rate except that for the same L/G ratio, the Peclet number increases with flow rate. A gas Peclet number, 417, was obtained for the 15.2-cm-ID column with no liquid in the column. The determination of this Peclet number is discussed in Appendix 10.4.

Axial dispersion was accounted for in the K_La calculation with an average Peclet number of 18. The variation of K_La with gas and liquid mass flux is presented in Fig. 10. There are insufficient data to provide a correlation. However, the data for gas fluxes of 1.62 and 0.46 x 10^{-2} gm/cm^2-sec suggest that K_La increases with the liquid flux and perhaps less so at larger gas fluxes. Difficulties in extracting gas samples from the column that were representative of the actual inlet and outlet concentrations led to poor closure of mass balances between the liquid and gas streams and the inability to calculate K_La for these experiments. This problem was especially severe with the 27.9-cm-ID column.

6. CONCLUSIONS

1. The 15.2-cm-ID column floods at lower gas flow rate than the 6.35-cm-ID column for the same liquid flow rate.

2. For L/G ratios greater than 20 and less than 400, there is an approximate linear relation between liquid and gas mass flow rates at which flooding occurs for both columns.

3. For the 6.35-cm-ID column the Goodloe correlation falls below the data on the generalized flooding correlation plot. There is better agreement between the Goodloe correlation and data for the 15.2-cm-ID column.

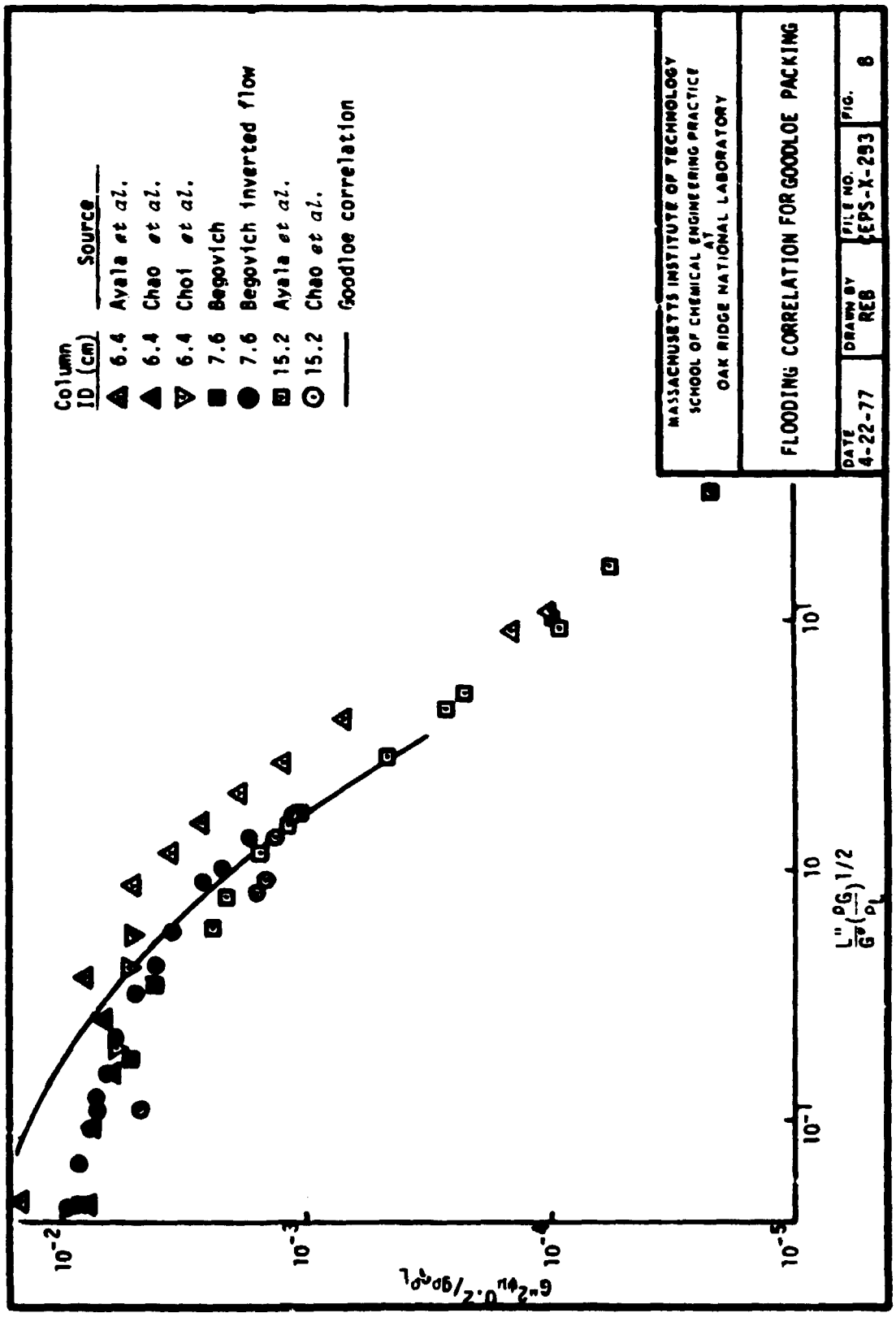
Column ID (cm)
Source
6.4 Ayala et al.
6.4 Chao et al.
6.4 Choi et al.
7.6 Begovich
7.6 Begovich inverted flow
15.2 Ayala et al.
15.2 Chao et al.
Goodloe correlation
MASSACHUSETTS INSTITUTE OF TECHNOLOGY
SCHOOL OF CHEMICAL ENGINEERING PRACTICE
AT
OAK RIDGE NATIONAL LABORATORY
FLOODING CORRELATION FOR GOODLOE PACKING
DATE 4-22-77
DRAWN BY REB
FILE NO. EPS-X-293
FIG. 8
10^{-2}
10^{-3}
10^{-4}
10^{-5}
10^{-1}
10^{1}
10
$G''^{2}\mu^{0.2}/g\rho_G\rho_L$
$\frac{L''}{G''}\left(\frac{\rho_G}{\rho_L}\right)^{1/2}$

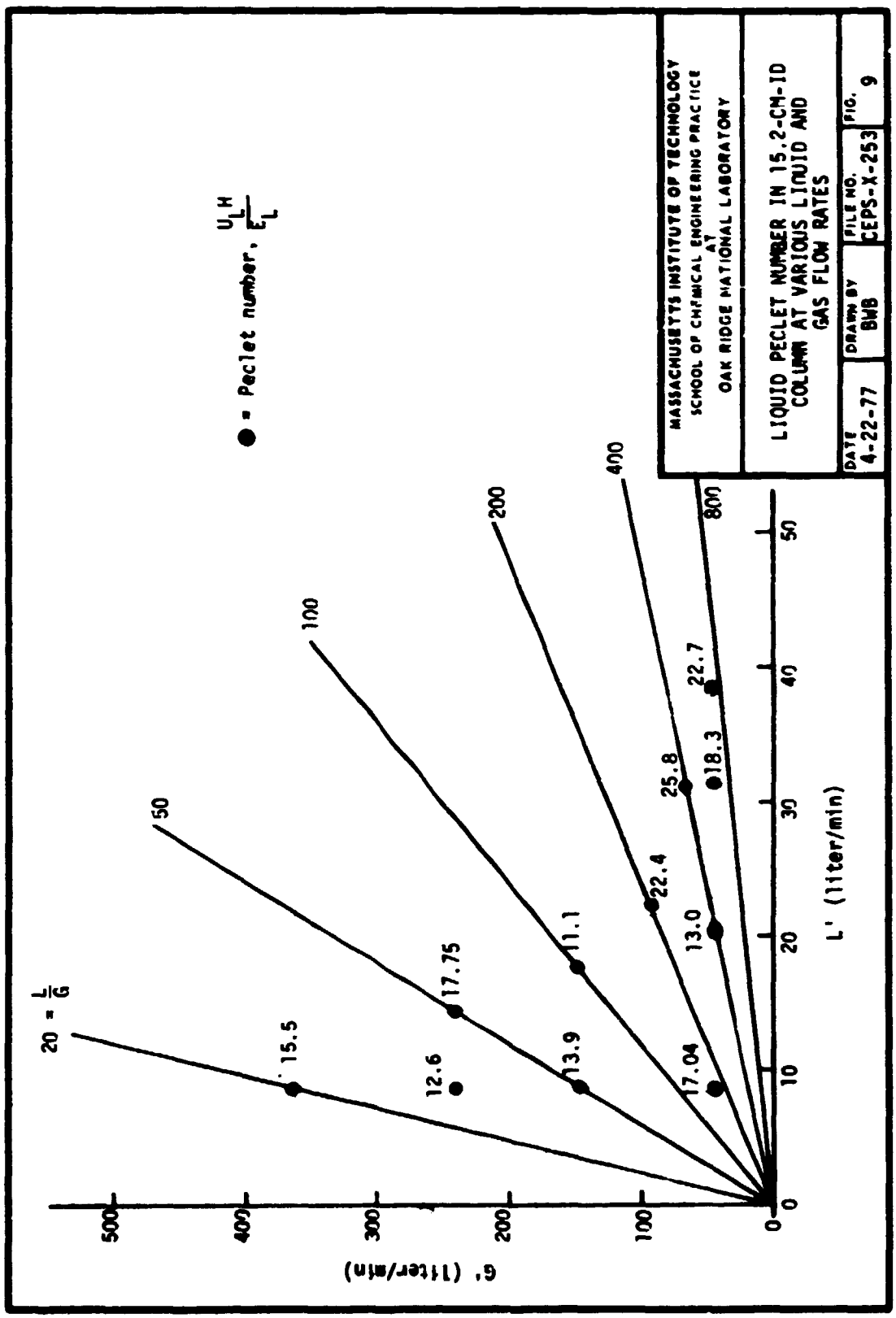
● = Peclet number, $\frac{U_L H}{E_L}$
$20 = \frac{L}{G}$
50
100
200
400
800
15.5
12.6
17.75
13.9
11.1
17.04
22.4
13.0
25.8
18.3
22.7
G' (liter/min)
L' (liter/min)
0
100
200
300
400
500
10
20
30
40
50
MASSACHUSETTS INSTITUTE OF TECHNOLOGY
SCHOOL OF CHEMICAL ENGINEERING PRACTICE
AT
OAK RIDGE NATIONAL LABORATORY
LIQUID PECLET NUMBER IN 15.2-CM-ID COLUMN AT VARIOUS LIQUID AND GAS FLOW RATES
DATE 4-22-77
DRAWN BY BMB
FILE NO. CEPS-X-253
FIG. 9

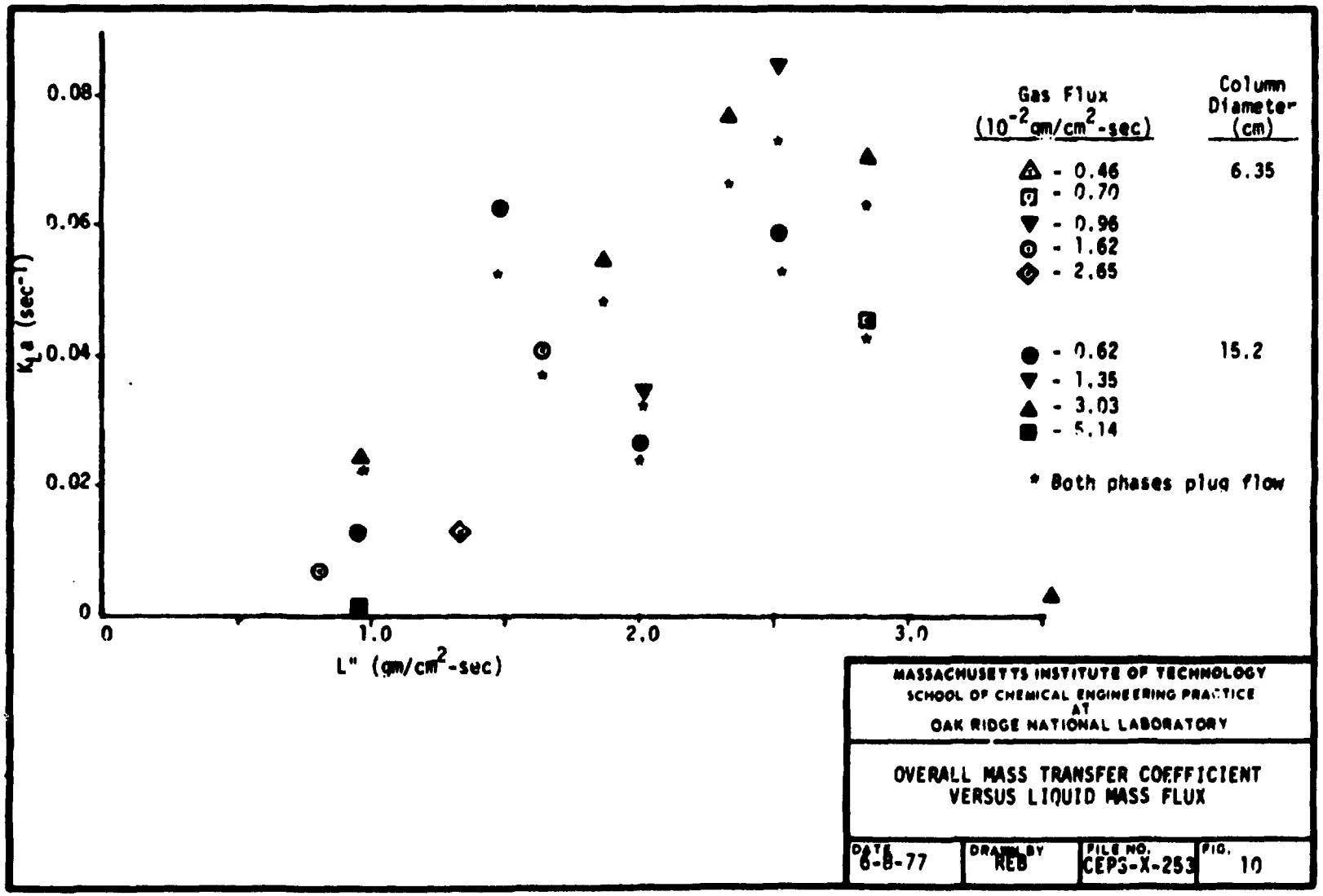
0.08
0.06
0.04
0.02
0
$K_L a$ (sec^{-1})
0
1.0
2.0
3.0
L" (gm/cm^2-sec)
Gas Flux
(10^{-2} gm/cm^2-sec)
Column Diameter (cm)
- 0.46
- 0.70
- 0.96
- 1.62
- 2.65
6.35
- 0.62
- 1.35
- 3.03
- 5.14
15.2
* Both phases plug flow
MASSACHUSETTS INSTITUTE OF TECHNOLOGY
SCHOOL OF CHEMICAL ENGINEERING PRACTICE
AT
OAK RIDGE NATIONAL LABORATORY
OVERALL MASS TRANSFER COEFFICIENT
VERSUS LIQUID MASS FLUX
DATE 6-8-77
DRAWN BY REB
FILE NO. CEPS-X-253
FIG. 10

4. The liquid Peclet number ranged from 11.1 at a liquid-to-gas mass flux ratio of 100 to 25.8 at a ratio of 400.

5. Insufficient data could be analyzed to provide a correlation between $K_L a$ and L" due to problems in extracting representative gas samples from the column. With an average liquid Peclet number of 18 and the plug flow assumption for the gas phase, $K_L a$ ranged from ~0.01 to 0.08 sec^{-1}.

7. RECOMMENDATIONS

1. Increase the water pumping capacity to 185 liter/min to obtain flooding data on the 27.9-cm-ID column.

2. Devise a means to accurately sample the gas inlet and outlet concentrations and gas and liquid concentration within the packing rather than at the column wall.

3. Perform tracer experiments with a non-absorbable gas such as helium to determine the gas phase Peclet number.

8. ACKNOWLEDGMENTS

We wish to thank our consultants, J.M. Begovich and A.D. Ryon, for advice on the project and to G.L. Haag for timely procurement of analytical equipment.

9. LOCATION OF DATA

Data for experiments are located in ORNL Databook A-7555-G, pp. 1-69, on file at the MIT School of Chemical Engineering Practice, Bldg. 3001, ORNL.

10. APPENDIX

10.1 Calculation of $K_L a$

$K_L a$ was calculated twice, once by assuming plug flow in both gas and liquid phases and once by assuming plug flow in the gas phase and axially dispersed flow in the liquid phase. Both solutions are presented in Miyauchi (9). For both phases in plug flow and F and λ defined as

$$F = \frac{mU_G}{U_L}$$

and

$$\lambda = -NTU_G(1 - F)$$

the solutions are

$$x = \frac{C_G - mC_L'}{1 - mC_L'} = \frac{e^{\lambda z_*} - Fe^{\lambda}}{1 - Fe^{\lambda}}$$

and

$$y = \frac{m(C_L - C_L')}{1 - mC_L'} = \frac{(e^{\lambda z_*} - e^{\lambda})F}{1 - Fe^{\lambda}}$$

At $z_* = 1$, the first expression can be rearranged to give

$$NTU_G = \frac{1}{1 - F} \ln \frac{1 - F + x_{z_*=1}F}{x_{z_*=1}}$$

where:

$$x_{z_*=1} = \frac{C_{GO} - mC_L'}{1 - mC_L'}$$

Alternatively, at $z_*=0$, the second expression can be rearranged to give

$$NTU_G = \frac{1}{1 - F} \ln \frac{Fy_{z_*=0} - F}{y_{z_*=0} - F}$$

where:

$$y_{z_*=0} = \frac{m(C_{LO} - C_L')}{1 - mC_L'}$$

NTU_G can then be calculated from experimentally determined inlet and outlet gas and liquid carbon dioxide concentrations.

For axially dispersed liquid flow and plug gas flow, NTU_G cannot be isolated in the solution; consequently, an iterative technique was employed by assuming NTU_G to be between 0 and 100 and using an interval halving convergence technique until the calculated value of x or y was within 0.001% of its experimentally determined outlet value at $z_*=1$ and 0, respectively. For

$$h = NTU_G + Pe_L$$

$$k = NTU_G\, Pe_L (1 - F)$$

$$\lambda_1 = 0$$

$$\lambda_2 = -\frac{h}{2} + \sqrt{\left(\frac{h}{2}\right)^2 - k}$$

$$\lambda_3 = -\frac{h}{2} - \sqrt{\left(\frac{h}{2}\right)^2 - k}$$

$$\bar{h}_i = 1 + \frac{\lambda_i}{NTU_G}$$

$$D_{H1} = \bar{h}_2\lambda_2(1 + \lambda_3/Pe_L)e^{\lambda_3}\bar{h}_3 - \bar{h}_3\lambda_3(1 + \lambda_2/Pe_L)e^{\lambda_2}\bar{h}_2$$

$$D_{H2} = \bar{h}_3\lambda_3$$

$$D_{H3} = -\bar{h}_2\lambda_2$$

$$D_H = D_{H1} + (\bar{h}_3\lambda_3 - \bar{h}_2\lambda_2)$$

and

$$H_i = D_{H_i}/D_H$$

the solut ons are

$$x = \sum_{i=1}^{3} H_i e^{\lambda_i z_*}$$

and

$$y = \sum_{i=1}^{3} \bar{h}_i H_i e^{\lambda_i z_*}$$

The computer listing for these calculations are given in Appendix 10.5.

10.2 Sample Calculations

10.2.1 Coordinates for Generalized Flooding Correlation

A general correlation on the performance of tower packing similar to that made by Eckert *et al.* (6) was made by plotting for each flooding point:

$$A' = \frac{G''^2 \psi \mu^{0.2}}{g \rho_G \rho_L} \text{ vs } B = \frac{L''}{G''}\left(\frac{\rho_G}{\rho_L}\right)^{1/2} = \frac{L}{G}\left(\frac{\rho_G}{\rho_L}\right)^{1/2}$$

For the air-carbon dioxide-water system,

$$\psi = 1.0$$

$$\mu = 1.3 \text{ cp}$$

$$\rho_G = 1.202 \times 10^{-3} \text{ gm/cm}^3$$

$$\rho_L = 1.0 \text{ gm/cm}^3$$

For the 15.2-cm-ID column, one flooding point was observed at an L' of 25.4 liter/min and a G' of 143 liter/min.

$$G'' = \frac{143 \text{ liter/min}(1000 \text{ cm}^3/\ell)(\text{min}/60 \text{ sec})(1.202\times10^{-3} \text{ gm/cm}^3)}{(15.2 \text{ cm})^2\pi/4}$$

$$= 1.579 \times 10^{-2} \text{ gm/cm}^2\text{-sec}$$

$$A' = \frac{(1.579 \times 10^{-2} \text{ gm/cm}^2\text{-sec})^2(1.3 \text{ cp})^{0.2}}{(981 \text{ cm/sec}^2)(1.202 \times 10^{-3} \text{ gm/cm}^3)(1.0 \text{ gm/cm}^3)}$$

$$= 2.228 \times 10^{-4} \text{ cm-cp}^{0.2}$$

$$L'' = \frac{(25.4 \text{ liter/min})(1000 \text{ cm}^3/\ell)(\text{min}/60 \text{ sec})(1.0 \text{ gm/cm}^3)}{(15.2 \text{ cm})^2\pi/4}$$

$$= 2.333 \text{ gm/cm}^2\text{-sec}$$

$$B = \frac{2.333}{1.579 \times 10^{-2}}\left(\frac{1.202 \times 10^{-3}}{1.0}\right)^{1/2} = 5.12$$

These A',B data points were then plotted on a log-log scale (see Fig. 8) and compared with previous work.

10.2.2 Manufacturer's Flooding Correlation

The following correlation is given by the manufacturer of Goodloe packing, the Packed Column Company (10):

$$U' = \frac{2.8712}{\mu^{0.33}}\left(\frac{\rho_L - \rho_G}{\rho_G}\right)^{0.57} = \frac{2.8712}{(1.3)^{0.33}}\left(\frac{1 - 1.202\times10^{-3}}{1.202 \times 10^{-3}}\right)^{0.57}$$

$$= 1.215 \times 10^2 \text{ cm/sec}$$

For L/G ratios not equal to 1, U' is corrected with a manufacturer's graph of correction factors vs L/G in a range of L/G from 0.1 to 100. For an L/G of 40, the correction factor is 0.28.

$$U_G = U'(\text{correction factor}) = 1.215 \times 10^2(0.28) = 34 \text{ cm/sec}$$

From U_G one then obtains the gas mass flow rate, G. For a 15.2-cm-ID column,

$$G = U_G(A)\rho_G = 34.0(182.46)(1.202 \times 10^{-3}) = 7.46 \text{ gm/sec}$$

The liquid mass flow rate for an L/G of 40 is

$$L = (\frac{L}{G})G = 40(7.46) = 298.4 \text{ gm/sec}$$

To convert to volume flow rates,

$$G' = G(\frac{1}{\rho}) = G(\frac{1 \text{ cm}^3}{1.202 \times 10^{-3} \text{ gm}})(\frac{60 \text{ sec}}{\text{min}})(\frac{\text{liter}}{1000 \text{ cm}^3}) = 372.4 \text{ l/min}$$

$$L' = L(1 \text{ cm}^3/\text{gm})(60 \text{ sec/min})(\text{liter}/1000 \text{ cm}^3) = 17.90 \text{ liter/min}$$

The manufacturer's correlation is plotted along with the experimental data on the general flooding correlation (Fig. 8).

10.3 Determination of Liquid Peclet Number

According to Levenspiel (7),

$$\sigma_\theta^2 = \frac{\sigma^2}{\bar{t}^2} = \frac{2}{Pe} - 2(\frac{1}{Pe})^2(1 - e^{-Pe})$$

With an experimentally obtained residence time distribution curve, σ_θ is evaluated numerically with the following set of equations:

$$\bar{t} = \frac{\Sigma t_i c_i \Delta t_i}{\Sigma c_i \Delta t_i}$$

$$\sigma^2 = \frac{\Sigma t_i^2 c_i \Delta t_i}{\Sigma c_i \Delta t_i} - \bar{t}^2$$

which combine to give,

$$\sigma_\theta^2 = \frac{(\Sigma t_i^2 c_i \Delta t_i)(\Sigma c_i \Delta t_i)}{(\Sigma t_i c_i \Delta t_i)^2} - 1$$

In the numerical analysis, the experimental curve was divided using the trapezoidal rule along intervals that very closely approximated the shape of the curve.

10.4 Basis for Plug Flow Assumption in the Gas Phase

Several gas phase residence time distribution, RTD, curves were obtained from a step input of carbon dioxide using a Beckman analyzer set to record the amount of carbon dioxide in the exit gas as a function of time. Taking the difference in the times for 16 and 84% of the input concentration to arrive at the detector gives two standard deviations around the mean residence time. Thus,

$$\sigma = \frac{t(84) - t(16)}{2}$$

$$\bar{t} = t(50)$$

$$\sigma_\theta = \frac{\sigma}{\bar{t}}$$

and

$$Pe = \frac{2}{\sigma_\theta^2}$$

From one RTD curve the standard deviation, σ, was 4.68 sec, the mean residence time was 67.5 sec, and the Peclet number was 417. This number was higher than it would be otherwise because of the distance between the location of the step input and the CO_2 analyzer.

The only case for which a gas RTD curve was obtained was with no liquid in the column. This is because carbon dioxide is absorbed by water and would yield misleading results. With the liquid flow, the gas Peclet number would be lower. Dunn *et al.* (5) have measured liquid and gas Peclet numbers in columns with 1-in. Berl saddles and 1- and 2-in. Raschig rings. In their study there was an inverse relationship between the void fraction of a particular packing and the Peclet number. Berl saddles, with a void fraction of 0.79, appeared closest of the three packings studied to Goodloe packing,

with a void fraction of 0.95 (4). At the same gas flow rate and no liquid flow rate, the gas Peclet number was 482 for 1-in. Berl saddles. The liquid Peclet numbers ranged from about 39 to 107 for 1-in. Berl saddles and were much higher for the 1- and 2-in. Raschig rings over the L/G range of interest. These values are approximately four times those obtained for Goodloe packing in the present study. Based on the above values, a rough estimate for gas Peclet numbers in the L/G range of interest from the gas Peclet numbers for the 1-in. Berl saddles in the same range can be obtained. The 1-in. Berl saddle gas Peclet numbers vary from 206 to 668, and the corresponding Goodloe packing gas Peclet numbers should be approximately one-fourth of this. With moderate error, then, plug flow can be assumed in the gas phase.

10.5 Computer Programs

Nomenclature:

AREA	column cross-sectional area, cm^2
CAVE	average concentration of an integration increment (mmho)
CGIN	inlet concentration of CO_2 in gas, gm/cm^3
CGOUT	outlet concentration of CO_2 in gas, gm/cm^3
CLIN	inlet concentration of CO_2 in liquid, gm/cm^3
CLOUT	outlet concentration of CO_2 in liquid, gm/cm^3
CXOUT	dimensionless outlet gas concentration
CYIN	dimensionless inlet liquid concentration
CYOUT	dimensionless outlet liquid concentration
JCOL	column diameter, cm
F	extraction factor FM*GV/LV
FG	gas mass flow rate, gm/sec
FKGAAX	gas phase mass transfer coefficient times interfacial area per unit volume assuming dispersed flow, sec^{-1}
FKGAPX	gas phase mass transfer coefficient times interfacial area per unit volume assuming plug flow, sec^{-1}
FKLAAX	liquid phase mass transfer coefficient times interfacial area per unit volume assuming dispersed flow, sec^{-1}

FKLAPX	liquid phase mass transfer coefficient times interfacial area per unit volume assuming plug flow, sec^{-1}
FL	liquid mass flow rate, gm/sec
FLG	liquid-to-gas mass flow ratio
FNOX	number of transfer units
FM	Henry's law constant
FSTAR	dimensionless distance along column
GV	gas flow rate, liter/min
H	column height, cm
HTUAX	height of transfer unit assuming dispersed flow, cm
HTUPX	height of transfer unit assuming plug flow, cm
LV	liquid flow rate, liter/min
N	number of increments in numerical integration
NTUXX	number of transfer units based on plug flow and outlet gas concentration
NTUXY	number of transfer units based on plug flow and outlet liquid concentration
NTUXXA	number of transfer units based on dispersed flow and outlet gas concentration
NTUXYA	number of transfer units based on dispersed flow and outlet liquid concentration
PE	inverse Peclet number
PEY	liquid phase Peclet number
SIGMA2	variance of RTD curve, sec^2
STHETA	dimensionless variance of RTD curve
TAVE	average time of an integration increment, sec
TBAR	average residence time, sec
UG	gas superficial velocity, cm/sec
UL	liquid superficial velocity, cm/sec

XOUT dimensionless outlet gas concentration

YOUT dimensionless outlet liquid concentration

10.5.1 Liquid Peclet Number Computation

```
C       THIS PROGRAM CALCULATES THE VARIANCE
C        AND AVERAGE RESIDENCE TIME GIVEN C AND T DATA POINTS.
C       FROM THIS INFORMATION THE PECLET NUMBER OF THE
C      SYSTEM CAN BE CALCULATED.
C
       DIMENSION T(50),C(50),DELTAT(50),CAVE(50)
       DIMENSION TAVE(50)
       TYPE 100
  100  FORMAT(7(/),1X,'ENTER THE NUMBER OF CONCENTRATION-
      1TIME POINT PAIRS TO BE USED')
       ACCEPT 200,N
       TYPE 101
101    FORMAT(1X,'ENTER EACH POINT PAIR IN TWO
      1 TEN SPACE FIELDS, TIME FIRST')
       DO 10 I=1,N
       ACCEPT 201,T(I),C(I)
10     CONTINUE
       DO 11 J=1,N-1
       DELTAT(J)=T(J+1)-T(J)
       CAVE(J)=(C(J+1)+C(J))/2.
       TAVE(J)=(T(J+1)+T(J))/2.
11     CONTINUE
       TBARN=0.
       TBARD=0.
       SIGMAN=0.
       DO 12 I=1,N-1
       TBARN=TBARN+TAVE(I)*CAVE(I)*DELTAT(I)
       TBARD=TBARD+CAVE(I)*DELTAT(I)
12     CONTINUE
       TBAR=TBARN/TBARD
       DO 13 I=1,N-1
       SIGMAN=SIGMAN+TAVE(I)*TAVE(I)*CAVE(I)*DELTAT(I)
13     CONTINUE
       SIGMA2=SIGMAN/TBARD-TBAR*TBAR
       STHETA=SIGMA2/(TBAR*TBAR)
200    FORMAT(I3)
201    FORMAT(2F10.4)
       PEU=100.
       PED=0.
       DO 14 I=1,200
       PE=(PEU+PED)/2.
       F=2.*PE-2.*PE*PE*(1.-EXP(-1./PE))
```

```
      TEST=F-STHETA
      IF(ABS(TEST).LE..000001) GOTO 36
      IF(TEST) 35,36,37
35    PED=PE
      GOTO 14
37    PEU=PE
14    CONTINUE
      TYPE 300,PE,F,TEST
300   FORMAT(1X,'CONVERGENCE FAILURE ON PE',3E14.6)
36    TYPE 400,TBAR,SIGMA2,STHETA,PE
400   FORMAT(1X,'TBAR=',F10.5,/,1X,'SIGMA2=',F10.5,
     1/,1X,'STHETA=',F10.5,/,1X,'PE=',F10.5)
      STOP
      END
```

10.5.2 Determination of $K_L a$

```
C     THIS PROGRAM CALCULATES THE VALUES OF KLA
C     GIVEN THE INLET AND OUTLET CONCENTRATIONS
C     ,THE FLOWRATES AND THE HENRY'S LAW CONSTANT
C
      REAL LV,NTUXX,NTUXY,NTUXXA,NTUXYA
      TYPE 99
99    FORMAT(1X,'ASSIGN A TWO DIGIT NUMBER TO THIS RUN')
      ACCEPT 333,IRUN
333   FORMAT(I2)
      TYPE 224
224   FORMAT(1X,'WHAT IS THE COLUMN HEIGHT IN CM')
      ACCEPT 465,H
465   FORMAT(F10.2)
      TYPE 188
188   FORMAT(/,/,/,/,/,1X,'ENTER CLIN,CLOUT,CGIN,CGOUT,
     1LV,GV,PEX,PEY,FM,AREA ',/1X,'FIVE
     2 TO A LINE.')
      TYPE 200,CLIN,CLOUT,CGIN,CGOUT,LV
      ACCEPT 210,CLIN,CLOUT,CGIN,CGOUT,LV
      TYPE 201,GV,PEX,PEY,FM,AREA
200   FORMAT(1X,4F10.8,F13.4)
201   FORMAT(1X,5F10.4)
210   FORMAT(4F10.8,F10.4)
211   FORMAT(5F10.4)
      ACCEPT 211,GV,PEX,PEY,FM,AREA
      FLG=LV/GV*831.95
      FG=GV/AREA*1.202/60.
      FL=LV/AREA*1000./60.
      DCOL=2.*SQRT(AREA/3.14159)
C
C     CALCULATE THE VALUE OF F
C
```

```
      F=FM*GV/LV
C
C     CALCULATE THE SUPERFICIAL VELOCITIES
C
      UL=LV/AREA*1000./60.
      UG=GV/AREA*1000./60.
C
C     CALCULATE DIMENSIONLESS CONCENTRATIONS AT
C     EACH END OF COLUMN
C
      CXOUT=CCOUT/CGIN
      CYIN=CLIN/CGIN
      CYOUT=CLOUT/CGIN
C
C     IN TERMS OF GENERALIZED CONCENTRATIONS
C
      XOUT=(CXOUT-FM*CYIN)/(1.-FM*CYIN)
      YOUT=(CYOUT-CYIN)*FM/(1.-FM*CYIN)
C
C     IF BOTH PHASES WERE IN PLUG FLOW
C
      ARGX=ABS((F*(XOUT-1.)+1.)/XOUT)
      ARGY=ABS((F*(YOUT-1.))/(YOUT-F))
      NTUXX=ALOG(ARGX)/(1.-F)
      NTUXY=ALOG(ARGY)/(1.-F)
C
C     IF BOTH PHASES ARE AXIALLY DISPERSED
C

       TUPX=100.
       TUPY=100.
       TDX=0.
       TDY=0.
       DO 10 I=1,200
       TX=(TUPX+TDX)/2.
       CALL DISP(X,Y,F,TX,PEY,1.)
       TEST=X-XOUT
       IF(ABS(TEST/XOUT).LE..00001) GOTO 36
       IF(TEST) 35,36,37
 35    TUPX=TX
       GOTO 10
 37    TDX=TX
 10    CONTINUE
       TYPE 400,X,XOUT,TX
 400   FORMAT(1X,'CONVERGENCE ON X CASE FAILED',/,1X
      1,3E14.6)
 36    DO 11 I=1,200
       TY=(TUPY+TDY)/2.
       CALL DISP(X,Y,F,TY,PEY,0.)
       TEST=Y-YOUT
       IF(ABS(TEST).LE..00001) GOTO 46
       IF(TEST) 45,46,47
```

```
45    TOY=TY
      GOTO 11
47    TUPY=TY
11    CONTINUE
      TYPE 588,Y,YOUT,TY
588   FORMAT(1X,'CONVERGENCE ON Y CASE FAILED',/,1X
     1,3E14.6)
46    NTUXXA=TX
      NTUXYA=TY
C
C     NOW KGA CAN BE CALCULATED FOR EACH CASE
C
      FKGAPX=UG/H=NTUXX
      FKGAPY=UG/H=NTUXY
      FKGAAX=UG/H=NTUXXA
      FKGAAY=UG/H=NTUXYA
C
C     IN TERMS OF KLA
C
      FKLAPX=FM=FKGAPX
      FKLAPY=FM=FKGAPY
      FKLAAX=FM=FKGAAX
      FKLAAY=FM=FKGAAY
C
C     FOR HTU'S IN EACH CASE WE HAVE
C
      HTUPX=H/NTUXX
      HTUPY=H/NTUXY
      HTUAX=H/NTUXXA
      HTUAY=H/NTUXYA
C
C     THAT'S IT ... OUTPUT TIME

C
      TYPE 111,IRUN,FLB,FG,FL,DCOL
111    FORMAT(/,/,//,/,/,/,1X,'RESULTS OF MASS TRANSFER
     1 RUN',I2,/,/,1X,'L/GB',F13.4,/,1X,'GFLUX=',F10.4,
     2' G/CM2-SEC',/,1X,'LFLUX=',F10.4,' G/CM2-SEC',
     3/,1X,'USING ',F10.2,'ID COLUMN',//,/,1X,
     4'CASE       NTJX         NTUY         HTJX         HTUY
     5         KGA          KLA    ',/)
      TYPE 112,NTUXX,NTUXY,HTUPX,HTUPY,FKGAPX,FKLAPX
112   FORMAT(1X,'PLUG-PLUG',1X,6F10.5)
      TYPE 114,NTUXXA,NTUXYA,HTUAX,HTUAY,FKGAAX,FKL
     1AAX
114   FORMAT(1X,'AXIL-AXIL',1X,6F10.5)
      STOP
      END
```

10.5.3 Listing of Subroutine DISP

```
C       THIS PROGRAM CALCULATES THE VALUES
C       OF X AND Y FOR THE CASE OF THE
C       LIQUID DISPERSED AND THE GAS IN
C       PLUG FLOW FOR EXTRACTION FACTORS
C       NOT EQUAL TO ONE.
C
        SUBROUTINE DISP(X,Y,F,FNOX,PEY,ZSTAR)
        DIMENSION H(3),FLA(3),HH(3)
        HS=FNOX*PEY
        FK=FNOX*PEY*(1.-F)
        FLA(1)=0.
        FLA(2)=-(HS/2.)+SQRT((HS/2.)*(HS/2.)-FK)
        FLA(3)=-(HS/2.)-SQRT((HS/2.)*(HS/2.)-FK)
        DO 10 I=1,3
        H(I)=1.+FLA(I)/FNOX
10      CONTINUE
        DH1=H(2)*FLA(2)*(1.+FLA(3)/PEY)*H(3)*EXP(FLA(3)
       1)*(H(3)*FLA(3)*(1.+FLA(2)/PEY)*H(2)*EXP(FLA(2)))
        DH=DH1-H(2)*FLA(2)*H(3)*FLA(3)
        DH2=H(3)*FLA(3)
        DH3=-H(2)*FLA(2)
        HH(1)=DH1/DH
        HH(2)=DH2/DH
        HH(3)=DH3/DH
        X=0.
        Y=0.
        DO 11 I=1,3
        Y=Y+H(I)*HH(I)*EXP(FLA(I)*ZSTAR)
        X=X+HH(I)*EXP(FLA(I)*ZSTAR)
11      CONTINUE
        RETURN
        END
```

10.6 Nomenclature

A	column cross-sectional area, cm^2
a	interfacial area per unit packed volume, cm^{-1}
A'	dimensionless ordinate on generalized flooding correlation, $G^{*2}\psi_\mu^{0.2}/g\rho_G\rho_L$
c_i	concentration of carbon dioxide in phase i, gm/cm^3
C_i	dimensionless concentration, $c_i(z_*)/c_G(0)$
B	dimensionless abscissa on generalized flooding correlation, $L/G(\rho_G/\rho_L)^{1/2}$

E_i axial dispersion coefficient for phase i, cm^2/sec

F extraction factor, mU_G/U_L

g acceleration due to gravity

G gas mass superficial velocity, gm/sec

G" gas mass flux, gm/cm^2-sec

G' gas volumetric flow rate, liter/min

H column height, cm

HTU_i height of transfer unit based on phase i, H/NTU_i

K_i transfer coefficient for phase i, cm/sec

L liquid mass superficial velocity, gm/sec

L" liquid mass flux, gm/cm^2-sec

L' liquid volumetric flow rate, liter/min

m Henry's law constant based on concentrations

NTU_i number of transfer units for phase i, $K_G aH/U_i$

Pe_i Peclet number in phase i, HU_i/E_i

P pressure, cm H_2O

ΔP pressure drop across the column, cm H_2O

t time, sec

$\bar{t}$ mean residence time, sec

Δt time interval, sec

T temperature, °K

U' uncorrected gas velocity in manufacturer's flooding correlation, cm/sec

U_i superficial velocity of phase i, cm/sec

x generalized gas phase concentration, $(C_G - mC_L') / (1 - mC_L')$

y generalized liquid phase concentration, $m(C_L - C_L') / (1 - mC_L')$

z distance along column, cm

z_* dimensionless column height, z/H

Greek Symbols

ρ density, gm/cm^3

μ viscosity, cp

θ dimensionless time, $t/\bar{t}$

σ^2 variance, sec^2

σ_θ^2 dimensionless variance

σ mean standard deviation, sec

Subscripts

i phase interface, numerical integration interval

G gas phase

L liquid phase

θ at dimensionless time

10.7 Literature References

1. Begovich, J.M., and J.S. Watson, "Flooding Characteristics of Goodloe Packing," ORNL-TM-5212, pp. 1-29 (January 1976).

2. Bragg, L.B., "Goodloe Column Packing: A New Knit Packing Material for Vapor Liquid Contacting Operations," Ind. Eng. Chem., 49, 1062 (1957).

3. Chao, E.I., R.J. Bertolami, J-L.P. Varlet, and G.R. Wilkes, "Flooding and Mass Transfer in Goodloe-Packed Columns," ORNL/MIT-234 (May 1976).

4. Choi, W.M., R.C. Michel, and L-L.P. Varlet, "Flooding in Columns Filled with High Efficiency Packings," ORNL/MIT-223 (February 1976).

5. Dunn, W.E., *et al.*, "Longitudinal Dispersion in Packed Gas-Absorption Columns," I&EC Fund., 16(1), 116 (1977).

6. Eckert, J.S., E.H. Foote, and L.F. Walter, "What Affects Packing Performance?" Chem. Eng. Progr., 62(1), 59 (1966).

7. Levelspiel, O., "Chemical Reaction Engineering," 2nd ed., pp. 253-298, Wiley, New York (1972).

8. Miyauchi, T., and T. Kikuchi, "Axial Dispersion in Packed Beds," Chem. Eng. Sci., 30, 346 (1975).

9. Miyauchi, T., "Longitudinal Dispersion in Solvent Extraction Columns: Mathematical Theory," UCRL-3911, Lawrence Radiation Laboratory, Berkeley (August 15, 1957).

10. Packed Column Co., "How to Design a Goodloe Column," Information Bulletin.

11. Watson, J.S., and H.D. Cochran, Jr., "A Simple Method for Estimating the Effect of Axial Backmixing on Countercurrent Column Performance," Ind. Eng. Chem., 10(1), 83 (1977).